ISSN 1027-5495. Functional Materials, 26, No.1 (2019), p. 16-22.
doi:https://doi.org/10.15407/fm26.01.16

The chemical, phase composition and optical properties of $Zn_xCd_{1-x}S$ films obtained by close spaced vacuum sublimation

***Yu.Yeromenko*[1], *A.Opanasyuk*[1], *A.Voznyi*[1], *I.Shpetnyi*[1], *Yu.Gnatenko*[2], *V.Grebinaha*[3]**

[1]Sumy State University, 2 Rymsky Korsakov Str., 40007 Sumy, Ukraine
[2]Institute of Physics, National Academy of Sciences of Ukraine, 46 Nauky Ave., 03028 Kyiv, Ukraine
[3]National Technical University of Ukraine "Kyiv Polytechnic Institute", 37 Peremogy Ave., 03056 Kyiv, Ukraine

Received October 31, 2018

The optical properties, chemical and phase composition of $Zn_xCd_{1-x}S$ films obtained by close-spaced vacuum sublimation (CSS) were studied using X-ray diffraction, energy dispersive X-ray analysis and optical spectroscopy methods. The solid solution films were deposited at the substrate and evaporator temperatures of T_s = 573 K and T_e = 1273 K, respectively. ZnS and CdS powders were mixed with different weight ratios (x = 0; 0.2; 0.4; 0.6; 0.8; 1.0) for further deposition of $Zn_xCd_{1-x}S$ films. It was found that the optical properties (band gap, transmission and absorption coefficients) of $Zn_xCd_{1-x}S$ films depends on the chemical composition and can be controlled by the weight percentages of the initial powders. It was found that the actual zinc concentrations in the films is higher than expected and the film thickness reduces with increasing of x. This results demonstrate that $Zn_xCd_{1-x}S$ solid solutions films obtained by CSS have improved optical parameters, high crystal quality and good stoichiometry.

Keywords: $Zn_xCd_{1-x}S$ films, vacuum sublimation, optical properties.

Изучены оптические свойства, химический и фазовый составы пленок $Zn_xCd_{1-x}S$, полученных вакуумным испарением в квазизамкнутом объеме. Пленки твердого раствора наносили при температурах подложки и испарителя T_s = 573 К и T_e = 1273 К соответственно. Для дальнейшего осаждения пленок $Zn_xCd_{1-x}S$ порошки ZnS и CdS смешаны в различных весовых соотношениях (x = 0; 0,2; 0,4; 0,6; 0,8; 1,0). Обнаружено, что оптические свойства (коэффициент пропускной способности, коэффициент пропускания и поглощения) пленок $Zn_xCd_{1-x}S$ зависят от их химического состава и могут регулироваться весовым составом исходной шихты. Установлено, что фактические концентрации цинка в пленках выше, чем ожидалось, а толщина пленок уменьшается с увеличением x. Эти результаты показывают, что тонкие слои твердого раствора $Zn_xCd_{1-x}S$, полученные методом КСО, имеют улучшенные оптические параметры, высокое качество кристаллов и хорошую стехиометрию.

Хімічний, фазовий склад та оптичні властивості плівок $Zn_xCd_{1-x}S$ одержаних вакуумним випаровуванням у квазізамкненому об'ємі. *Ю.С.Єрьоменко, А.С.Опанасюк, А.А.Возний, І.О.Шпетний, Ю.П.Гнатенко, В.І.Гребинаха.*

Вивчено оптичні властивості, хімічний та фазовий склад плівок $Zn_xCd_{1-x}S$, отриманих вакуумним випаровуванням у квазізамкненому об'ємі (КЗО). Плівки твердого розчину нанесено при температурах підкладки і випарника T_s = 573 К та T_e = 1273 К відповідно. Для подальшого осадження плівок $Zn_xCd_{1-x}S$ порошки ZnS та CdS змішані

у різних вагових співвідношеннях (x = 0; 0,2; 0,4; 0,6; 0,8; 1,0). Виявлено, що оптичні властивості (коефіцієнт пропускної здатності, коефіцієнт пропускання та поглинання) плівок $Zn_xCd_{1-x}S$ залежать від їх хімічного складу і можуть регулюватися ваговим складом вихідної шихти. Встановлено, що фактичні концентрації цинку у плівках вищі, ніж очікувалося, а товщина плівок зменшується зі збільшенням x. Ці результати показують, що тонкі шари твердого розчину $Zn_xCd_{1-x}S$, отримані методом КЗО, мають поліпшені оптичні параметри, високу якість кристалів і хорошу стехіометрію.

1. Introduction

In recent years, the interest of scientists in new semiconductor materials with specific properties has increased. Semiconductor thin films are widely used as the functional layers in optoelectronic and photovoltaics devices. Therefore, deposition of the thin films with optimal optical characteristics, there is one of the most important tasks for researchers [1, 2].

Today, the most common devices in photovoltaics are silicon-based. Thin films heterojunction solar cells can be attractive alternative. In photovoltaic cells with CdTe, $Cu(In,Ga)Se_2$ (CIGS) and some other absorber layers cadmium sulphide (CdS) is traditionally used as a window layer [3–5]. However, replacement of CdS layer is also considered today. One of the most promising candidates for window layer replacement is $Zn_xCd_{1-x}S$ [6]. Solid solutions thin films have superior optical characteristics. At the same time, adjusting Zn content allows to regulate band gap and lattice parameters [7]. It provides increased transmission of the window layer in wide wavelength range, and the recombination losses decreasing at the boundaries of the contacting materials.

$Zn_xCd_{1-x}S$ thin films can be fabricated using a number of methods, such as: spray pyrolysis [8,9], chemical bath deposition, dip coating, and others [10]. However, it is well known that semiconductor layers with the best characteristics are usually obtained by vacuum methods [1, 2]. Among them, close-spaced sublimation (CSS) is one of the most attractive. This method allows to obtain high purity semiconductor films, with controlled growth conditions and optimal structural, optical and electrical characteristics [2, 11]. Therefore, CSS method was chosen for $Zn_xCd_{1-x}S$ thin films producing.

The structural and optical properties of CdS and ZnS films, deposited by CSS, were studied in the works [12–16]. However, the properties of $Zn_xCd_{1-x}S$ films, obtained by CSS method, have not been studied well enough. The purpose of this work is to investigate the influence of the growth conditions on the elemental compositions, structural and optical properties of CSS-evaporated $Zn_xCd_{1-x}S$ thin films.

2. Experimental

$Zn_xCd_{1-x}S$ solid solutions thin films were obtained in a VUP-5M vacuum chamber by close-spaced sublimation. It was grown the two series of samples at similar conditions: on glass (for X-ray diffraction and surface analysis) and on ITO coated glass substrates (for optical characteristics and elemental composition investigations, with further study of electrical properties). In both cases, the substrates were cleaned using isopropyl alcohol, and afterwards annealed in vacuum.

Among deposition parameters, the two has huge effect on the films properties, namely substrate (T_s) and evaporator (T_e) temperatures [2, 11]. This temperatures were set to T_s = 573 K and T_e = 1273 K, respectively. As a source material for $Zn_xCd_{1-x}S$ deposition was composed of ZnS and CdS powders that were mechanically mixed with the different weight proportions (x = 0; 0.20; 0.40; 0.60; 0.80; 1.0). In all cases, 1 mg of powder was evaporated. The weight percentage of ZnS and CdS powders were evaluated using the precision weights. This has allowed us to obtain pure films of initial materials, and solid solutions films with different Zn percentages. Details of close-spaced sublimation technique are described in [14].

The method of investigating the structural characteristics and elemental composition of the CSS-evaporated films of II–VI compound solid solutions ($Cd_{1-x}Zn_xTe$) is described in [17]. X-ray diffraction (XRD) method was used for the phase composition investigations. The measurements were carried out in the range of $2\theta = 25°–120°$ (2θ — is the Bragg angle), using DRON 4-07 diffractometer, with Ni-filtered Cu K_α radiation and Bragg-Brentano focusing. Phase analysis of $Zn_xCd_{1-x}S$ films was performed by comparing interplanar distances and relative intensities of the investigated films and the references JCPDS [18–20].

Scanning electron microscopy method (REM-100) was used to carry out the surface morphology investigations. The average

grain sizes of the samples were estimated by using Jeffries formula:

$$D = k\sqrt{S_0 / M^{-2} n_g}, \quad (1)$$

where k — is the coefficient of grain shape; S is the area of the micrograph region; M is the magnification; n_g is the number of grains on the selected region.

The elemental composition of $Zn_xCd_{1-x}S$ films was studied using the energy dispersive X-ray (EDX) analysis equipped to scanning electron microscope (REM-106i). We determined the atomic concentrations of the elements in $Zn_xCd_{1-x}S$ solid solutions and also calculated the relative concentration of zinc (x). To prevent misinterpretation of the results of chemical analysis, the background spectrum of substrate was subtracted.

The optical studies were carried out at the room temperature by SolidSpec-3700 UV-VIS-NIR spectrophotometer in the wavelength range $\lambda = (300–1500)$ nm. The transmittance spectrum $T(\lambda)$ was measured considering the substrates spectral properties. First of all, we obtained ITO-coated glass substrates basic spectrum. Afterwards it was automatically subtracted. The illumination was performed from $Zn_xCd_{1-x}S$ film side.

In spectral distributions of transmission coefficient $T(\lambda)$, we have observed interference fringes due to the multiple reflections of the two film interfaces. This indicates that the films prepared under the experimental conditions are smooth and uniform. These interference peaks are used to determine the film thickness, which is calculated using the following formula [21]:

$$d = \frac{\lambda_1 \lambda_2}{2n(\lambda_2 - \lambda_1)}, \quad (2)$$

where $\lambda_{1,2}$ is the wavelengths of two adjacent minimums of maximums; n is the refractive coefficient of material, which was taken from the reference [21]. In each case, calculations of the films thickness have been carried out using the value of the first two maxima.

The absorption spectra of $Zn_xCd_{1-x}S$, required for optical band gap E_g calculations, was calculated using Lambert-Beer law:

$$\alpha = -\frac{1}{d} \ln T, \quad (3)$$

where T is the optical transmittance; d is the thickness of the film.

The optical band gap of the material has been determined using the formula for the semiconductors with direct band gap energy [21]:

$$\alpha h\nu = A_0 (h\nu - E_g)^{1/2}, \quad (4)$$

where A_0 is the constant dependent on the charge carriers effective mass in the material; $h\nu$ is the photon energy.

It follows, that the optical band gap E_g can be defined by extrapolation of the linear part of $(\alpha h\nu)^2 - h\nu$ plot onto the $h\nu$ (energy axis).

3. Results and discussion

The visual inspection revealed that $Zn_xCd_{1-x}S$ films were optically transparent and homogeneous.

XRD patterns of the obtained films showed in Fig. 1a. As a result of XRD-analysis it was determined, that depending on different elemental compositions of the layers, (002) peaks from hexagonal phase of CdS or (111) peaks from cubic phase of ZnS were dominant. Moreover, when $x > 0$, the diffraction peaks shift toward the higher 2θ values relatively to pure CdS (Fig. 1b). This indicates that obtained films are actually present solid solutions of the specified materials, also witnessing of the lattice microstrains [22]. It was found that in CSS-evaporated $Zn_xCd_{1-x}S$ films a phase transition from the hexagonal to the cubic structure is occurring at $x \geq 0.8$. A similar phenomenon was observed in the other works, where composition dependence of structural properties was studied [23–25].

SEM images of the films surface showed in Fig. 2. The layers consist of grains with very different sizes. The average grain size varied from 0.85 μm for CdS to 1.15 μm for ZnS, respectively. In general, CSS deposited $Zn_xCd_{1-x}S$ films grain sizes is much larger, than chemically deposited layers, where average grain sizes does not exceed 0.1 μm [8–10]. Larger crystalline sizes lead to reduced interface recombination, increased lifetimes and larger mean free path of the charge carriers. It improves also optical properties of the films and should allow increasing the efficiency of solar cells [13–14]. The transmittance spectrum dependences of the samples with different Zn concentration are presented in Fig. 3a. The appearance of interference fringes indicates that the surface of prepared films is homogeneous and smooth.

As can be seen in Fig. 3a, films has the high transmittance in a wide wavelength

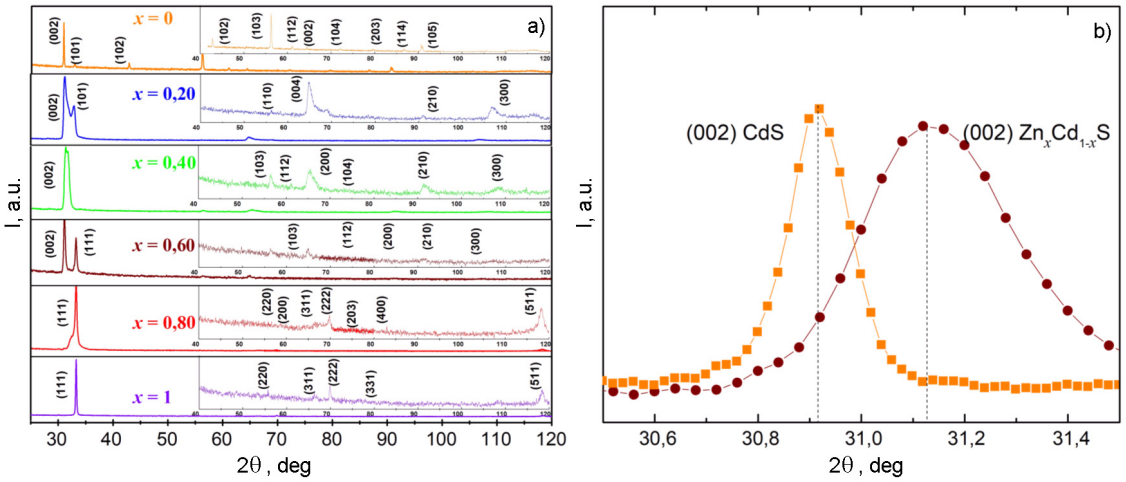

Fig. 1. XRD patterns of $Zn_xCd_{1-x}S$ films with different weight concentration of zinc x in initial powder (a) and shift in (002) peek positions of $Zn_xCd_{1-x}S$ (weight concentration $x = 0.60$), relatively CdS ($x = 0$) (b).

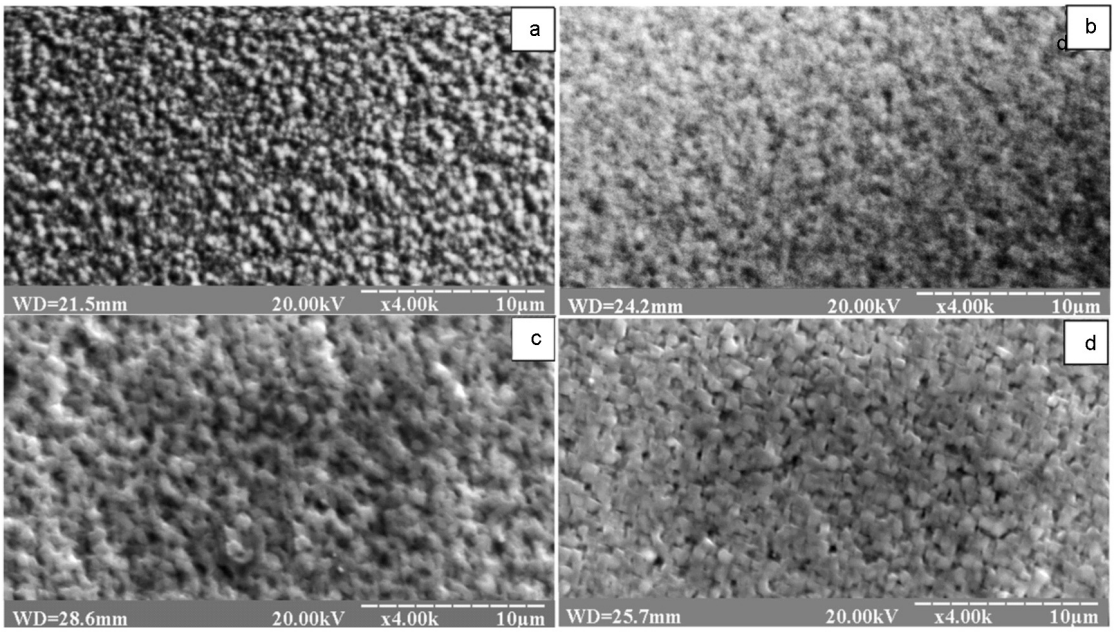

Fig. 2. SEM images of the $Zn_xCd_{1-x}S$ films with different weight concentration of zinc x in initial powder: 0 (a); 0.40 (b); 0.60 (c); 1 (d).

range. As expected, the lowest transmittance has pure CdS ($x = 0$) sample, having the largest thickness of the film, and the smallest optical band gap value. The best transmittance has pure ZnS and $Zn_xCd_{1-x}S$ solid solutions thin films. Regarding the interference, the maximum transmittance was observed for the layers with $x = 1$ ($\lambda = 410$ nm, $T = 98.3$ %) and $x = 0.4$ ($\lambda = 655$ nm, $T = 97.52$ %). However, the average transmittance increased with elevated Zn content and decreased film thicknesses. Also, it was observed, that ZnS and CdS shows high transmittance in a narrow wavelength range, while $Zn_xCd_{1-x}S$ films have $T > 70$ % in a wide wavelength range. It can be explained by the fact, that while every initial material has best transmittance in various spectral ranges, their solid solutions films have the properties of both materials superimposed.

The transmittance coefficients values were used to calculate and plot the optical absorption spectrum using formula (3). The spectral distribution of the absorption coefficients α chartered in Fig. 3b. As can be seen, there is a tendency to reduced α with increasing of zinc weight concentration (x), when $\lambda = \text{const}$. The best absorption was ob-

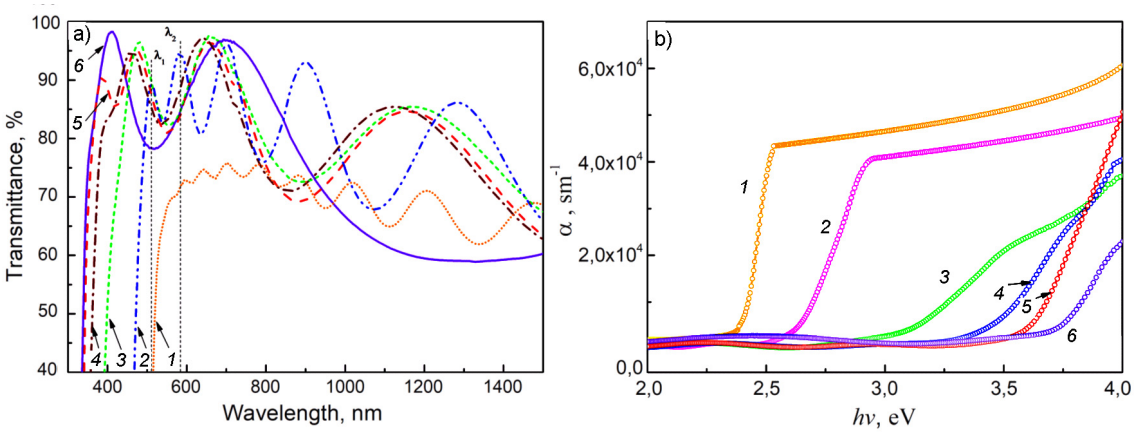

Fig. 3. Optical transmission spectra (a) and absorption spectra (b) for $Zn_xCd_{1-x}S$ films with different weight concentration of zinc x in initial powder: 0 (*1*); 0.20 (*2*); 0.40 (*3*); 0.60 (*4*); 0.80 (*5*); 1 (*6*).

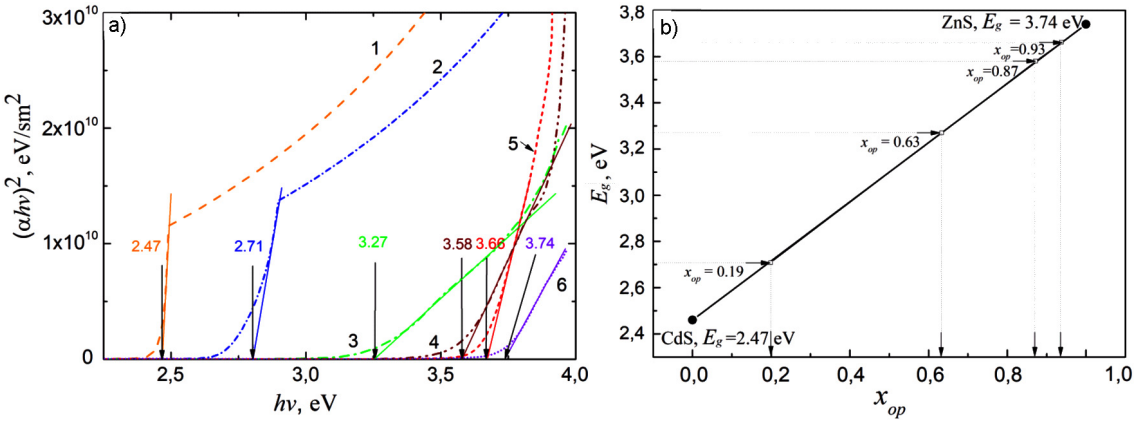

Fig. 4. $(\alpha h\nu)^2 - h\nu$ dependences (a) and determination of zinc concentration (x_{op}) by band gap values (b) of the $Zn_xCd_{1-x}S$ films with different weight concentration of zinc x in initial powder: 0 (*1*); 0.20 (*2*); 0.40 (*3*); 0.60 (*4*); 0.80 (*5*); 1 (*6*).

served for pure CdS films, the worst — for pure ZnS films. The absorption in higher-lying band gap region was $\alpha = (2{\cdot}10^4 – 4{\cdot}10^4)$ m^{-1}.

To determine optical band gap of material E_g using the dependences on Fig. 3b, $(\alpha h\nu)^2 - h\nu$ graphs were plotted. The linear parts of these graphs were extrapolated to the photon energy axis. The point of intersection with the axis gives us the optical band gap energy E_g. The results of band gap determination for CdS, ZnS, and their solid solutions are presented in Fig. 4a. The analysis of the results shows, that band gap of investigated films varied in the range from $E_g = 2.47$ eV (CdS, $x = 0$) to $E_g = 3.74$ eV (ZnS, $x = 1$).

The calculated values of optical band gap are in a good agreement with the reference data [26, 27]. In the work [26] for films prepared by spray-pyrolysis, band gap varied from $E_g = 2.44$ eV for CdS to $E_g = 3.75$ eV for ZnS. The band gap of sintered $Zn_xCd_{1-x}S$ ($x = 0 – 1$) films varied from 2.44 to 3.50, respectively [27]. Moreover, in all cases was observed increasing E_g with zinc content growth.

Afterwards the determined E_g values were used to estimate real zinc concentrations in the films (x_{op}) by the Vegard's law (Fig. 4b) [28, 29]. The results are presented in the Table. It was found, that chemical composition was significantly different than expected from weight concentrations of initial powders. It was observed that zinc concentrations x_{op} was higher, than expected.

Further, EDX method was used for more precise investigations of the elemental composition. The results of elemental composition investigations by different methods and stoichiometry ($C_{(Zn+Cd)}/C_S$) summarized in the Table. As we can see from the Table, the results of EDX measurements correlate with optical investigations values x_{op}. However, there is some discrepancy between two methods for $x = 0.20$ and $x = 0.40$ zinc weight concentrations in the initial powder. This can be explained as result of the

Table. The results of $Zn_xCd_{1-x}S$ films investigations

x	E_g	x_{op}	x_{EDX}	Zn	Cd	S	C_{Zn+Cd}/C_S
Expected from Zn weight concentration	eV	Determined from E_g	Determined by EDX method	at. %	at. %	at. %	
0	2.47	0	0	–	49.93	50.06	1.00
0.20	2.71	0.19	0.36	17.30	33.51	49.19	1.03
0.40	3.27	0.63	0.74	35.69	13.37	50.94	0.96
0.60	3.58	0.87	0.88	41.01	6.02	52.97	0.89
0.80	3.66	0.93	0.95	44.78	2.53	52.69	0.90
1.00	3.74	1.00	1.00	46.95	–	53.05	0.89

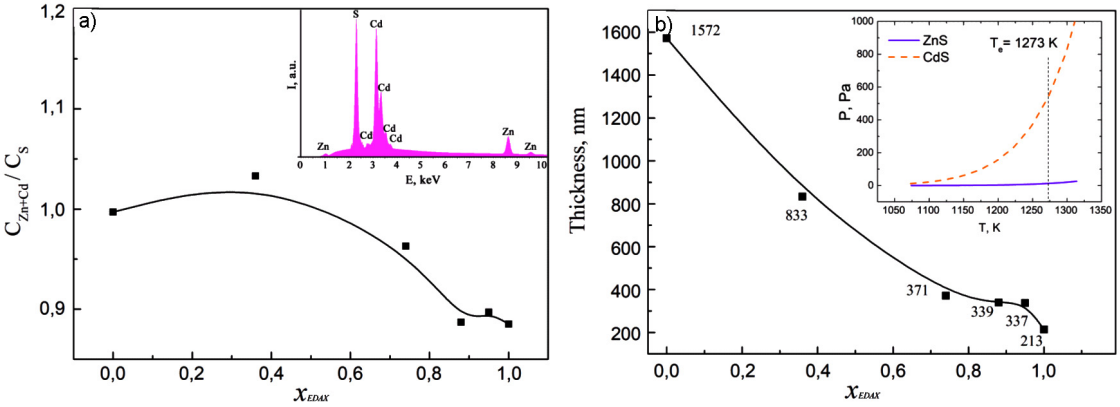

Fig. 5. The dependence of the films stoichiometry C_{Zn+Cd}/C_S on zinc content x_{EDX}, which was indicated by EDX method (a) and thickness of $Zn_xCd_{1-x}S$ films with different zinc concentrations x_{EDX} (b). The typical characteristic EDX spectra of $Zn_xCd_{1-x}S$ solid solutions films and dependences of ZnS and CdS gas pressure on temperature are presented on insets.

Vegard's law for E_g determination, instead of using more complex and accurate non-linear model [30] and measurements from different points on the film. In Fig. 5a showed the dependence of the films stoichiometry on zinc content (x_{EDX}). As we can see from the Figure, the films with x_{EDX} = 0–0.50 is close to stoichiometric. At the same time, the samples with $x_{EDX} > 0.50$ have some excess of sulphur.

As indicated above, the interference fringes in the dependence of the transmission coefficient on wavelength were used to calculate the films thickness. The results of appropriate calculations are presented in Fig. 5b. We plotted film thickness versus x_{EDX} values, because EDX method is the most accurate. Thickness of obtained films decreased with increasing the zinc content from 1.57 μm to 213 nm (Fig. 5b). This can be explained by the features of evaporation process in vacuum. Initial powder consists of mixing CdS and ZnS compounds. ZnS gas pressure is much smaller than CdS gas pressure (inset in Fig. 5b). Therefore, with increasing of zinc concentration flux density of evaporated substance and film thickness is decreased.

4. Conclusions

The elemental, phase composition and optical properties of $Zn_xCd_{1-x}S$ films obtained by CSS were studied. It was found, that optical band gap of the deposited films increased from E_g = 2.47 eV (CdS) to 3.74 eV (ZnS) with increasing of zinc content x from 0 to 1. The values of zinc concentrations determined from EDX analysis is in good agreement with values obtained from optical studies. However, concentrations were significantly different in comparison with the initial weight concentrations. The stoichiometry of the films is also affected by Zn concentration and varied from 1.00 (x = 0) to 0.89 (x = 1).

We have observed the tendency of the increase of transmission coefficients of the $Zn_xCd_{1-x}S$ films with increasing zinc concentration. Also, solid solutions films have better transmittance in wide range of the

spectrum, than initial CdS and ZnS. The optical interference fringes observed in the transmission spectra were used to calculate the thickness of $Zn_xCd_{1-x}S$ films. It was showed that the films thicknesses were reduced with the increase of x in the range of 1.57 μm to 213 nm. The analysis of the experimental data allows us to conclude that $Zn_xCd_{1-x}S$ solid solutions films have improved optical characteristics.

Therefore, $Zn_xCd_{1-x}S$ films deposited by CSS at conditions to T_s = 573 K and T_e = 1273 K showed the promising physical and optical properties to use as the novel window layer for second (CdTe, CIGS) and third (CZTS) generation thin film solar cells.

Acknowledgements. This work was supported by the Ministry of Education, Science of Ukraine (Grants No. 0116U002619 and 0116U006813).

References

1. S.Adachi, Handbook on Physical Properties of Semiconductors V.3. II–VI Compound Semiconductors, Kluwer Academic Publishers, New York, Boston, (2004).
2. C.J.Panchal, A.S.Opanasyuk, V.V.Kosyak et al., *J. Nano-Electron. Phys.*, **3(1)**, 274 (2011).
3. J.Poortman, V.Arkhipov, Thin Film Solar Cells Fabrication, Characterization and Applications (2006).
4. A.Voznyi, Y.Yeromenko, V.Kosyak et al., in: Proc. 2017 IEEE 7th Intern. Conf. on Nanomaterials: Applications and Properties, NAP 2017, 03NE18-1 (2017).
5. R.Luo, B.Liu, X.Yang et al., *Appl. Surf. Sci.*, **360**, 744 (2016).
6. M.S.Hossain, N.Amin, M.A.Matin et al., *Chalcogenide Lett.*, **8, 263 (2011).**
7. V.Kumar, A.Sharma, D.K.Sharma et al., *Optik (Stuttg).*, **125**, 1209 (2014).
8. V.S.Raja, U.Chalapathi, S.Uthanna, *Opt.-Int. J. Light Electron Opt.*, **106**, 106 (2012).
9. Y.Raviprakash, K.V.Bangera, G.K.Shivakumar, *Sol. Energy*, **83**, 1645 (2009).
10. N.Roushdy, A.M.Farag, M.Abdel Rafea et al., *Superlat. Microstruct.*, **62**, 97 (2013).
11. A.Lopez-Otero, *Thin Solid Films*, **49**, 3 (1978).
12. D.I.Kurbatov, A.S.Opanasyuk, S.M.Duvanov et al., *Solid State Sci.*, **13**, 1068 (2011).
13. D.Kurbatov, V.Kosyak, A.Opanasyuk et al., *Phys. B Condens. Matter*, **404**, 5002 (2009).
14. D.Kurbatov, A.Opanasyuk, H.Khlyap, *Phys. Status Solidi Appl. Mater. Sci.*, **206**, 1549 (2009).
15. E.M.Feldmeier, A.Fuchs, J.Schaffner et al., *Thin Solid Films*, **519**, 7596 (2011).
16. C.Mejia-Garcia, A.Escamilla-Esquivel, G.Contreras-Puente et al., *J. Appl. Phys.*, **86**, 3171 (1999).
17. Y.V.Znamenshchykov, V.V.Kosyak, A.S.Opanasyuk et al., *Functional Materials*, **23**, 1 (2016).
18. B.E.Warren, X-ray Diffraction, Dover, New York (1990).
19. International Centre for Diffraction Data, USA, Card Number 00-036-1450.
20. International Centre of Diffraction Data, USA, Card Number 000-41-1049.
21. T.S.Moss, M.Balkanski, Handbook on Semiconductors: Optical Properties of Semiconductors, Elsevier, Amsterdam (1994).
22. W.Mahmood, N.A.Shah, *Opt. Mater. (Amst).*, **36**, 1449 (2014).
23. G.K.Padam, G.L.Malhotra, S.U.M.Rao, *J. Appl. Phys.*, **63**, 770 (1988).
24. R.Zia, F.Saleemi, S.Naseem, *Int. J. Mater. Res.*, **101**, 316 (2010).
25. E.F.El-Wahidy, A.A.M.Farag, M.A.Rafea et al., *Mater. Sci. Semicond. Process.*, **24**, 169 (2014).
26. M.C.Baykul, N.Orhan, *Thin Solid Films*, **518**, 1925 (2010).
27. V.Kumar, V.Singh, S.K.Sharma et al., *Opt. Mater. (Amst).*, **11**, 29 (1998).
28. J.Singh, Optoelectronics: An Introduction to Materials and Devices, Tata McGraw Hill New Delhi, (1996).
29. V.V.Kosyak, A.S.Opanasyuk, P.V.Koval et al., *J. Nano-Electron. Phys.*, **3**, 48 (2011).
30. G.Kartopu, A.J.Clayton, W.S.M.Brooks et al., *Prog. Photovoltaics Res. Appl.*, **20**, 6 (2012).